Absence of CD9 Enhances Adhesion-Dependent Morphologic Differentiation, Survival, and Matrix Metalloproteinase-2 Production in Small Cell Lung Cancer Cells

Yoshiyuki Saito, Isao Tachibana, Yoshito Takeda, Hiroyuki Yamane, Ping He, Mayumi Suzuki, Seigo Minami, Takashi Kijima, Mitsuhiro Yoshida, Toru Kumagai, Tadashi Osaki, and Ichiro Kawase

Department of Respiratory Medicine, Allergy and Rheumatic Diseases, Osaka University Graduate School of Medicine, Osaka, Japan

Abstract

While adhering to extracellular matrix proteins *in vitro* and *in vivo*, small cell lung cancer (SCLC) cells frequently show morphologic differentiation and are protected from apoptosis. Integrin β_1–mediated protein phosphorylation is suggested to be an essential signaling event in these processes. CD9 is an almost ubiquitously expressed tetraspanin protein that suppresses tumor progression by regulating cell motility and signaling through complex formation with β_1 integrins. We reported previously that, among tetraspanins, CD9 is selectively absent in most SCLC cells and that ectopic expression of CD9 suppresses their motility. Here, we show that the ectopic expression of CD9 suppressed neurite-like process outgrowth and promoted apoptotic death of SCLC cells that were adherent to fibronectin in serum-starved conditions. This correlated with attenuation of adhesion-dependent phosphorylation of Akt but not that of focal adhesion kinase or c-Jun NH_2-terminal kinase. Treatment of $CD9^-$ parent cells with a phosphatidylinositol 3-kinase (PI3K) inhibitor, LY294002, inhibited process outgrowth and survival, suggesting that PI3K/Akt signaling is required for the morphologic change and cell survival. Production of matrix metalloproteinase (MMP)-2 was likewise suppressed in the CD9 transfectants and in LY294002-treated parent cells. These results suggest that the absence of CD9 in SCLC cells may contribute to postadhesive morphologic differentiation, survival, and MMP-2 production via PI3K/Akt pathway. (Cancer Res 2006; 66(19): 9557-65)

Introduction

Lung cancer is classified into non–small cell lung cancer (NSCLC) and highly malignant small cell lung cancer (SCLC). The prognosis of SCLC patients is poor when compared with NSCLC patients. SCLC metastasizes to regional lymph nodes and distant organs extremely early; moreover, although SCLC initially responds to conventional chemotherapy and radiotherapy, a portion of tumor cells survives these treatments and grows into recurrent tumors (1). Resistance to the therapies seems to correlate with the appearance of morphologically variant tumor cells that have acquired antiapoptotic signals (2, 3). It was shown recently that SCLC cells are surrounded by a dense stroma of extracellular matrix (ECM) at primary and metastatic sites *in vivo* and that these ECM proteins protect SCLC cells from apoptosis through integrin-mediated signaling (3). The phosphatidylinositol 3-kinase (PI3K)/Akt signaling is most likely one such pathway that confers resistance to apoptosis. SCLC cell lines seemed to have constitutively elevated levels of PI3K activity, and PI3K inhibitors induced apoptosis of SCLC cells cultured in serum-free medium (4). Adherent SCLC cells converted from a floating type showed elevated activities of Akt and mitogen-activated protein kinase and acquired resistance to chemotherapeutic agents and radiation *in vitro* (5). Adhesion to fibronectin induced neurite-like projections and enhanced viability through the PI3K pathway in a SCLC line (6). In addition, SCLC cell adhesion to laminin caused flattened, epithelial cell morphology and increased Akt activation and cell survival after serum withdrawal (7). However, detailed mechanisms involved in such prominent activation of PI3K/Akt pathway in SCLC have yet to be determined.

The tetraspanin proteins comprise at least 32 members, including CD9, CD37, CD53, CD63, CD81, CD82, and CD151, in mammals. They are characterized by the structure that spans the plasma membrane four times and have a propensity to form complexes with each other and with other molecules, including integrins, signaling proteins, and membrane-anchored growth factors at tetraspanin-enriched microdomains (8). Among tetraspanins, CD9 and CD82 are considered to function as metastasis suppressors in solid tumors (9). Clinical and pathologic findings indicate that down-regulation of these tetraspanins correlates with progression of NSCLC and other cancers, including breast, pancreas, colon, and prostate. Reduced expression of the tetraspanins is more frequently observed in metastatic lesions than primary tumors, and patients with tumors lacking these tetraspanins are at advanced stages and show poor survival (10). Based on the facts that experimental transfection of CD9 and CD82 inhibited cell motility *in vitro* and tumor metastasis *in vivo*, it is believed that by modulating integrin functions these tetraspanins render cells more static and thus prevent tumor invasion and metastasis (11). However, it remains unclear whether down-regulation of these tetraspanins elicits antiapoptotic signals and promotes tumor cell survival. Of note, recent studies suggested that tetraspanins could influence adhesion-dependent signaling events, including activation of PI3K/Akt signaling. It was reported that, to control invasive migration, integrin-tetraspanin complexes may rearrange actin cytoskeleton and modulate matrix metalloproteinase (MMP)-2 production by PI3K-dependent mechanisms (12). In addition, ectopic expression of tetraspanins may exert a negative effect on adhesion-dependent activation of extracellular signal-regulated kinase (ERK) 1/2 and Akt (13). The implication of

Requests for reprints: Isao Tachibana, Department of Respiratory Medicine, Allergy and Rheumatic Diseases, Osaka University Graduate School of Medicine, 2-2 Yamada-oka, Suita, Osaka 565-0871, Japan. Phone: 81-6-6879-3833; Fax: 81-6-6879-3839; E-mail: itachi02@imed3.med.osaka-u.ac.jp.

doi:10.1158/0008-5472.CAN-06-1131

PI3K/Akt pathway in tetraspanin-mediated signaling raises a possibility that the expression of tetraspanins may have an effect not only on cell motility but also on cell survival or apoptosis.

We reported previously that the tetraspanin CD9 is expressed in most NSCLC cell lines, whereas it is absent in the majority of SCLC lines and SCLC tissues and that ectopic expression of CD9 suppresses integrin β_1–dependent motility of SCLC cells *in vitro* (14). These results suggest that the absence of CD9 may influence integrin-mediated postadhesive signaling events in SCLC. In this study, we investigated whether the absence of CD9 also affects survival of SCLC cells. Our data suggest that the CD9 absence contributes to morphologic change and prolongs survival of SCLC cells in serum-deprived conditions via the activation of PI3K/Akt signaling. The PI3K/Akt pathway also plays a role in the production of MMP-2 by $CD9^-$ SCLC cells.

Materials and Methods

Cell lines. OS3-R5 and OS2-RA were established in our laboratory, and their biological properties were characterized previously (14). OC10 and CADO LC6 were provided by Osaka Medical Center for Cancer and Cardiovascular Diseases (Osaka, Japan). NCI-H446 was purchased from the American Type Culture Collection (Rockville, MD). All cell lines were maintained in RPMI 1640 supplemented with 10% heat-inactivated fetal bovine serum (FBS), 100 units/mL penicillin, and 100 μg/mL streptomycin.

Antibodies and reagents. Anti-phosphorylated Akt (Ser^{473}), anti-Akt, and anti-phosphorylated c-Jun NH_2-terminal kinase (JNK) polyclonal antibodies were purchased from Cell Signaling Technology (Beverly, MA). Anti-phosphorylated focal adhesion kinase (FAK) polyclonal antibody and anti-CD9 monoclonal antibody (mAb; MM2/57) were from Biosource International (Camarillo, CA). Anti-FAK and anti-JNK1 polyclonal antibodies and anti-integrin α_v mAb (P2W7) were from Santa Cruz Biotechnology (Santa Cruz, CA). Anti-NAG-2 mAb (2E12) was described previously (15). Anti-integrin β_1 subunit mAb (4B4) was obtained from Beckman Coulter (Miami, FL). LY294002, PD98059, SB203580, and SP600125, which were specific inhibitors for PI3K, MEK1, p38, and JNK, respectively, were purchased from Calbiochem (San Diego, CA). Recombinant human stromal cell–derived factor-1α (SDF-1α) was purchased from Biosource International.

cDNA transfection. Establishment of stable CD9 and mock transfectants of OS3-R5 was described previously (14). A NAG-2 transfectant of OS3-R5 was established by transfection with NAG-2 cDNA in pCDM8 vector (15) using LipofectAMINE 2000 reagent (Invitrogen, Carlsbad, CA). Transient transfection of OS3-R5 and CADO LC6 with green fluorescent protein (GFP)–tagged CD9 (GFP-CD9) and GFP alone was described previously (14).

Flow cytometry. Cells (10^4) were incubated with 10 μg primary mouse mAbs and labeled with FITC-conjugated goat anti-mouse immunoglobulin (Biosource International). Normal mouse IgG was used as a control. Stained cells were analyzed on a FACScan (Becton Dickinson, San Jose, CA).

Cell adhesion assay. A 96-well nontissue culture-treated plate (Linbro, McLean, VA) was precoated with 20 μg/mL human plasma fibronectin (Sigma-Aldrich, St. Louis, MO). Nonspecific binding sites were blocked with PBS containing 0.1% bovine serum albumin (BSA). Cells (2.5×10^4) resuspended in serum-free RPMI 1640 containing 0.1% BSA were allowed to adhere to the fibronectin-coated wells for 1.5 hours in the presence of 5 μg/mL mAbs. Unattached cells were removed, and the remaining adherent cells were evaluated using a 3-(4,5-dimethylthiazol-2-yl)-2,5-diphenyltetrazolium bromide (MTT) assay as described previously (16).

Cell viability assay. Cells (3×10^5) were plated on a 24-well poly-L-lysine (PLL; Sigma-Aldrich)–coated or fibronectin-coated plate in serum-free (0.1% BSA) RPMI 1640 and cultured for 72 hours. Viable cells were quantified by the MTT assay or counted by trypan blue dye exclusion, and the percentage of viable cells was determined.

Process outgrowth assay. Cells (7×10^4) were seeded on a 24-well PLL- or fibronectin-coated plate in serum-free (0.1% BSA) RPMI 1640 and cultured for 3 or 24 hours. The cells were photographed, and the percentage of cells with a process longer than 1-cell diameter was determined (16). Cells transfected with GFP or GFP-CD9 were seeded on fibronectin-coated Lab-Tek glass chamber slides (Nunc, Rochester, NY) and cultured for 6 hours in the serum-free conditions. After fixation with 4% paraformaldehyde, images of fluorescent cells were obtained using a fluorescence microscope (Axioskop 2, Carl Zeiss, Thornwood, NY), and the percentage of process-bearing cells was determined as above.

Apoptosis assay. Cells (5×10^4) were seeded on PLL- or fibronectin-coated chamber slides and cultured for 48 hours in low-serum (0.1% FBS) RPMI 1640. The cells were fixed in 4% paraformaldehyde, and terminal deoxynucleotidyl transferase–mediated dUTP nick end labeling (TUNEL) was done using *In situ* Cell Death Detection kit, POD (Roche Diagnostics, Mannheim, Germany) according to the manufacturer's directions. The cells were counterstained with hematoxylin, and the percentage of apoptotic cells was determined.

Immunoblotting. After 24 hours of serum starvation, cells resuspended in serum-free (0.1% BSA) RPMI 1640 were plated for 0.5 to 48 hours on fibronectin-coated dishes or cultured for 5 to 30 minutes on nontissue culture-treated dishes in the presence of 100 ng/mL SDF-1α. The cells were lysed in radioimmunoprecipitation assay buffer containing 20 mmol/L Tris-HCl (pH 7.4), 150 mmol/L NaCl, 2 mmol/L EDTA, 1% NP40, 1% sodium deoxycholate, 0.1% SDS, 1 mmol/L phenylmethylsulfonyl fluoride, 10 μg/mL aprotinin, 10 μg/mL leupeptin, 1 mmol/L sodium orthovanadate, and 50 mmol/L NaF. Cell lysates were separated by 10% SDS-PAGE under reducing conditions, transferred to Immobilon-P membranes (Millipore, Bedford, MA), and probed with primary antibodies followed by peroxidase-conjugated donkey anti-rabbit IgG (Amersham, Piscataway, NJ). Immunoreactive bands were visualized with a chemiluminescent reagent (Perkin-Elmer, Boston, MA).

Small interfering RNA transfection. NCI-H446 cells (6.5×10^5) were cultured for 24 hours on a fibronectin-coated 6-cm dish and transfected with either 40 nmol/L cocktail small interfering RNA (siRNA) against human CD9 (SHF27A-0631, B-Bridge International, Sunnyvale, CA) or negative control cocktail RNAs (S30C-0126, B-Bridge International) using LipofectAMINE 2000 reagent. The cells were cultured for 72 hours on fibronectin in low-serum (1% FBS) RPMI 1640, and gene silencing effect was analyzed by immunoblotting for CD9.

Reverse transcription-PCR. Total RNA was extracted with Isogen (Nippon Gene, Tokyo, Japan) from cells cultured for 48 hours on fibronectin-coated dishes in serum-free (0.1% BSA) RPMI 1640. Total RNA (1 μg) was reverse transcribed with a cDNA synthesis kit (Invitrogen) using random hexamers. The thermal cycling variables were 35 cycles of 30 seconds at 94°C, 30 seconds at 66°C, and 60 seconds at 72°C for MMP-2, MMP-9, membrane-type MMP-1 (MT1-MMP), tissue inhibitor of metalloproteinase (TIMP)-1, and TIMP-2 and 25 cycles of 40 seconds at 94°C, 40 seconds at 60°C, and 90 seconds at 72°C for β-actin. We confirmed that these variables yielded amplification of template DNAs within a linear range. The sequences of upstream and downstream oligonucleotide primers were described previously (17).

Gelatin zymography. Cells (8×10^5) were plated on fibronectin-coated dishes in serum-free RPMI 1640 containing 25 mmol/L HEPES and cultured for 48 hours. The culture medium was concentrated 10-fold using Microcon (Millipore) and subjected to SDS-PAGE through 10% polyacrylamide gels containing 0.1% gelatin (Invitrogen). The gels were washed with 2.5% Triton X-100 and incubated in Novex zymogram developing buffer (Invitrogen). Lytic bands were visualized by staining with Coomassie brilliant blue R250.

Statistical analysis. All assays were done in triplicate cultures and values are expressed as mean ± SD. The statistical significance of differences was evaluated by ANOVA with Bonferroni's tests used for post hoc analyses. *P*s < 0.05 were considered statistically significant.

Results

Morphologic alteration and survival of SCLC cells after integrin-mediated adhesion. By an adhesion assay, we screened multiple SCLC lines and selected five lines that were adherent to

fibronectin. NCI-H446 was $CD9^+$ and the other four cell lines were $CD9^-$ (Fig. 1) as we showed previously by flow cytometry (14). Their adherence to fibronectin was uniformly blocked by anti-integrin β_1 mAb, indicating that β_1 integrins mediate cytoskeletal reorganization as major receptors for fibronectin (Fig. 1*A*). Anti-CD9 mAb did not affect the adhesion of $CD9^+$ NCI-H446. The morphologic change and survival of these cells were examined under serum-deprived culture conditions (Fig. 1*B*). When cultured for 24 hours, fibronectin induced these cells to extend long neurite-like projections. Meanwhile, on PLL, OS3-R5 and OC10 cells attached to the well but remained round. NCI-H446 cells adhered and spread on PLL but did not extend as long processes as fibronectin. On the other hand, CADO LC6 and OS2-RA cells on PLL not only spread but also extended projections as long as on fibronectin. These observations were confirmed when quantified as the percentage of process-bearing cells (Fig. 1*C, top*). The morphologic alterations seemed to be associated with prolonged cell survival. Cell viability was evaluated by a MTT assay after 72 hours of culture, and viable cells in OS3-R5, OC10, and NCI-H446 significantly increased on fibronectin, which enhanced their cell-shape change compared with PLL. Meanwhile, fibronectin did not increase viable cells in CADO LC6 and OS2-RA, which displayed no difference in morphology between PLL and fibronectin (Fig. 1*C, middle*). Cell viability was also evaluated by trypan blue dye exclusion, and results similar to the MTT assay were obtained (data not shown). Consistent with the increase in cell survival, fibronectin prevented apoptotic cell death, which was determined by TUNEL, in OS3-R5, OC10, and NCI-H446 (Fig. 1*C, bottom*).

Expression of CD9 reduces process outgrowth and cell survival in OS3-R5. Because OS3-R5 showed completely integrin β_1–dependent adherence to fibronectin and marked postadhesive morphologic change compared with PLL, we used this cell line in further experiments. As described above, OS3-R5 was $CD9^-$ under floating conditions and no CD9 expression was induced after 48-hour adherence to fibronectin even in 50 cycles of reverse transcription-PCR (RT-PCR; data not shown). To study effects of ectopic CD9 expression on the morphology and cell survival, we established stable transfectants that express CD9 (OS3-R5-CD9; ref. 14) and another tetraspanin, NAG-2 (OS3-R5-NAG-2). Flow cytometry data of these transfectants were shown in Fig. 2*A*. OS3-R5-CD9hi cells expressed a high level of CD9, whereas OS3-R5-CD9lo cells expressed less CD9, the level of which was comparable with that of the transfectant expressing NAG-2. These three transfectants, a mock transfectant, and the parent cell expressed similar levels of integrin α_v and β_1 subunits. α_3, α_4, and α_5 subunits were not expressed in these cells (data not shown). Coimmunoprecipitation experiments using the CD9 transfectant (Fig. 2*B*)

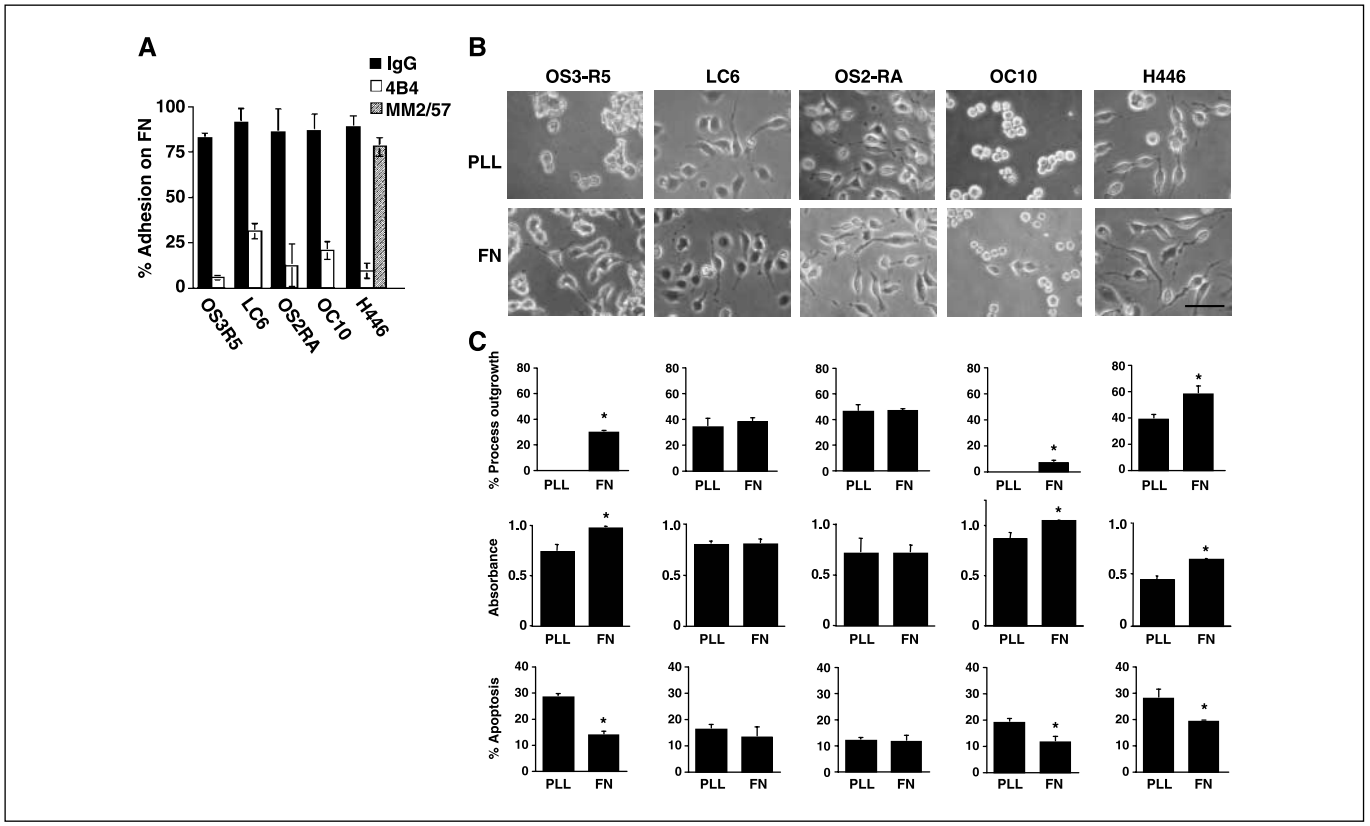

Figure 1. Integrin β_1–mediated morphologic differentiation and survival of SCLC cells. *A,* SCLC cells suspended in serum-free medium were allowed to adhere to fibronectin (*FN*)–coated wells for 1.5 hours in the presence of control IgG, anti-integrin β_1 mAb, 4B4, or anti-CD9 mAb, MM2/57. After nonadherent cells were removed by washing, remaining adherent cells were evaluated by a MTT assay. Percentage of the absorbance obtained from unwashed wells. *B,* SCLC cells were cultured for 24 hours on PLL- or fibronectin-coated wells in serum-free (0.1% BSA) medium and then photographed. Bar, 50 μm. *C,* cells were cultured for 24 hours as in (*B*), and the percentage of cells with a process longer than 1-cell diameter was determined (*top*). Cells were cultured for 72 hours as in (*B*), and viable cells were quantified by the MTT assay (*middle*). Cells were cultured for 48 hours on fibronectin-coated chamber slides in low-serum (0.1% FBS) conditions. After fixation, TUNEL was done and the percentage of apoptotic cells was determined (*bottom*). *Columns,* mean; *bars,* SD. *, $P < 0.05$. Levels of CD9 expression in flow cytometry were 1.2-fold (OS3-R5), 1.2-fold (CADO LC6), 1.2-fold (OS2-RA), 1.0-fold (OC10), and 87-fold (NCI-H446) when compared with control IgG.

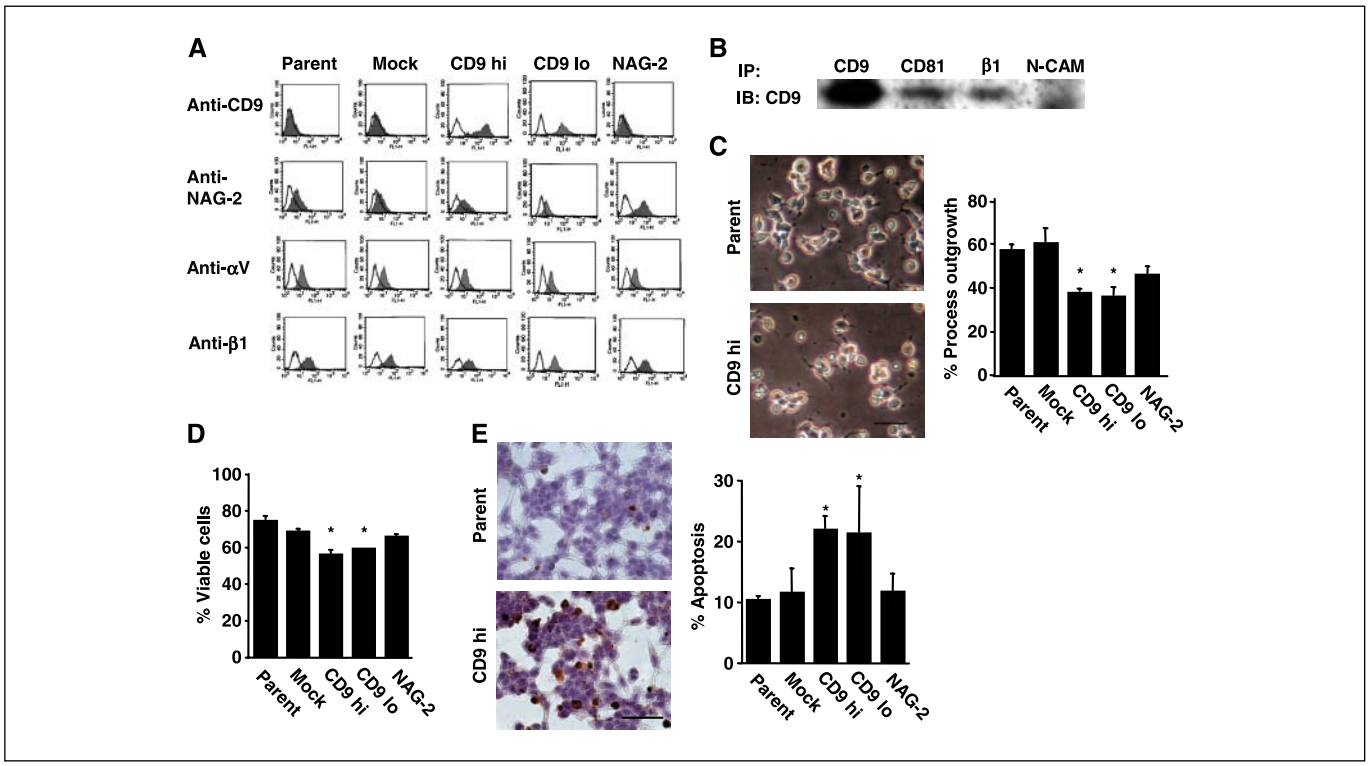

Figure 2. Decreased process outgrowth and increased apoptosis in CD9 transfectants of OS3-R5. *A,* OS3-R5 and its transfectants were stained with mAbs against CD9, NAG-2, integrin α_v, and integrin β_1, labeled with FITC-conjugated goat anti-mouse immunoglobulin, and analyzed on a FACScan (*shaded histograms*). *Open histograms,* staining with control IgG. When compared with control IgG, the levels of CD9 were 69- and 16-fold in OS3-R5-CD9hi and OS3-R5-CD9lo, respectively, and the level of NAG-2 was 14-fold in OS3-R5-NAG-2. *B,* OS3-R5-CD9lo cells were lysed with 1% Brij 99 lysis buffer. Immunoprecipitation (*IP*) was done by incubating lysates with mAbs against the indicated antigens. Precipitated proteins were separated by SDS-PAGE and transferred to a membrane, and immunoblotting (*IB*) was done with anti-CD9 mAb, MM2/57 (14). *C,* cells were cultured for 3 hours on fibronectin-coated wells in serum-free conditions. The cells were then photographed (*left*) and the percentage of cells with a process longer than 1-cell diameter was determined (*right*). *D,* cells were cultured for 72 hours as in (*C*). Viable cells were counted by trypan blue dye exclusion, and the percentage of viable cells was determined. *E,* cells were cultured for 48 hours on fibronectin-coated chamber slides in low-serum (0.1% FBS) conditions. After fixation, TUNEL was done and the cells were counterstained with hematoxylin (*left*). The percentage of apoptotic cells was also determined (*right*). Bar, 50 μm. *Columns,* mean; *bars,* SD. *, $P < 0.05$ versus parent.

showed that CD9 associates with its closely related tetraspanin, CD81, and β_1 integrins but not with N-CAM as we showed previously (14).

We seeded these cells onto fibronectin and the cells were exposed to serum-free conditions. In agreement with the similar levels of integrins (Fig. 2*A*), initial adherence to fibronectin, which was assessed 1.5 hours after plating by an adhesion assay, was not different among these cell lines (data not shown). However, when cultured longer (~3 hours), morphologic change, which was characterized by neurite-like projections, was observed in parent cells and mock transfectants, whereas this morphologic differentiation was partially but significantly impaired in OS3-R5-CD9hi and OS3-R5-CD9lo cells (Fig. 2*C*). The percentage of process-bearing OS3-R5-NAG-2 cells was also slightly lower than that of the parent cells, but this was not statistically significant. Associated with the defective morphologic differentiation, viable cells of OS3-R5-CD9hi and OS3-R5-CD9lo were decreased at 72 hours after plating as evaluated by trypan blue dye exclusion (Fig. 2*D*). The percentage of apoptotic cells, which was determined by TUNEL, was inversely elevated in the CD9 transfectants. The majority of TUNEL-positive cells were round (Fig. 2*E*). Thus, the expression of CD9, but not NAG-2, inhibits morphologic differentiation and induces early apoptosis in OS3-R5.

Expression of CD9 attenuates postadhesive phosphorylation of Akt. Of pathways activated by integrin-ECM binding, phosphorylation of FAK, Akt, ERK, and JNK were involved in integrin-mediated cytoskeletal reorganization and cell survival (18, 19). These signaling pathways were analyzed in OS3-R5 and its transfectants. As shown in Fig. 3*A*, FAK and JNK were constitutively phosphorylated and its level increased to similar extents after attachment to fibronectin in all cell lines, although the elevation of phosphorylated FAK seemed to be marginally attenuated in CD9 transfectants. Meanwhile, neither constitutive nor postadhesive phosphorylation of ERK1/2 was detected (data not shown). Akt was constitutively phosphorylated and its phosphorylation level increased until 90 minutes after adhesion in the parent, mock, and NAG-2 transfectants. Notably, this elevation of phosphorylated Akt was weak and transient in the CD9 transfectants. Indeed, the intensity of phosphorylated Akt band returned to the basal (floating condition) level after 90 minutes in OS3-R5-CD9hi cells. To examine if this attenuated Akt phosphorylation is specific to cell adherence, floating cells were stimulated with SDF-1α, a CXC chemokine that induces Akt phosphorylation through binding to its receptor, CXCR4 (Fig. 3*B*). Consistent with the time course reported previously (20), Akt was phosphorylated within 15 minutes of SDF-1α simulation, and this up-regulation of phosphorylated Akt was similar in all cell lines, indicating that phosphorylating machinery for Akt is intact in the CD9 transfectants. These cells expressed similar levels of CXCR4 in semiquantitative RT-PCR (data not shown).

We further examined fibronectin-induced Akt phosphorylation in a different time scale and confirmed that phosphorylated Akt was not elevated even after 6 to 24 hours of culture in OS3-R5-CD9hi cells (Fig. 3*C*). The level of phosphorylated Akt at 24 hours was rather lower than the basal (floating condition) level at 0 hour, possibly indicating the loss of constitutively active phosphorylated Akt, which might be induced by cell aggregate formation under floating conditions.

Transient expression of GFP-CD9 attenuates morphologic differentiation and Akt phosphorylation in SCLC cells. To exclude the possibility that the results from the CD9 transfectants were phenotypic variation among clones, we transiently transfected OS3-R5 and another CD9$^-$ SCLC line, CADO LC6, with GFP and GFP-CD9 and cultured them on fibronectin in serum-deprived conditions. Intracellular fluorescence distribution was analyzed after fixation (Fig. 4*A*). GFP-CD9 was distributed at the cell periphery and cell-cell contacts, whereas GFP displayed homogenous distribution; these were similar to the previously reported distribution in serum-containing conditions (14). Although filopodia formation seemed not to be different, long neurite-like protrusions were less marked in cells expressing GFP-CD9 when compared with cells expressing GFP alone in both OS3-R5 and CADO LC6 (Fig. 4*B*). Moreover, despite transient transfection, postadhesive Akt phosphorylation seemed to be attenuated in both cell lines (Fig. 4*C, top*). We additionally transfected another SCLC line, OC10, and GFP-CD9 again attenuated phosphorylation of Akt (Fig. 4*C, bottom*). Process extension by CADO LC6 and OC10 occurred relatively late (6-24 and 24-48 hours after plating, respectively; ref. 16) compared with OS3-R5 (~3 hours after plating). The late suppression of Akt phosphorylation in CADO LC6 and OC10 expressing GFP-CD9 may be related to this slow progression in morphologic differentiation.

Down-regulation of endogenous CD9 enhances Akt phosphorylation in a CD9$^+$ SCLC line. Exogenous expression of CD9 into CD9$^-$ SCLC cells attenuated postadhesive phosphorylation of Akt. To examine if inhibition of endogenous CD9 expression conversely enhances Akt phosphorylation in CD9$^+$ SCLC cells, we transfected siRNAs against CD9 into NCI-H446 cells cultured on fibronectin. As shown in Fig. 4*D*, after 72 hours of the siRNA transfection, CD9 was successfully reduced, and this was associated with enhancement of Akt phosphorylation in two independent experiments.

PI3K/Akt signaling is required for morphologic differentiation and cell survival of OS3-R5. Akt is a principal downstream effector of PI3K, and the PI3K/Akt pathway is one of key mediators in integrin-triggered signals (18). To address the role of the PI3K/Akt pathway in morphologic change and cell survival, parent OS3-R5 cells were treated with a synthetic PI3K inhibitor, LY294002, and other kinase inhibitors in serum-free conditions (Fig. 5*A*). LY294002 abolished the phosphorylation of Akt but did not affect that of FAK and JNK. SP600125, an inhibitor for JNK, completely inhibited phosphorylation of JNK but did not affect that of FAK and Akt. PD98059 and SB203580, specific inhibitors for MEK1 and p38, respectively, influenced none of FAK, Akt, and JNK phosphorylation when compared with vehicle alone. Treatment of these kinase inhibitors revealed no effect on initial cell adhesion to fibronectin in a 1.5-hour adhesion assay (data not shown). When OS3-R5 cells were cultured longer (~3 hours) in serum-deprived conditions, we noticed that the presence of DMSO somewhat disturbed process extension (compare % process outgrowth of OS3-R5 in Fig. 5*B* with that in Fig. 2*C*). Nonetheless, only LY294002 further inhibited the process outgrowth (Fig. 5*B*). Cell survival was also reduced by 50% at 72 hours of culture (Fig. 5*C*), and apoptotic cells were inversely increased 2.5-fold (Fig. 5*D*) by LY294002. SP600125 slightly decreased viable cells and increased apoptotic cells, but the effects were not statistically significant. Thus, OS3-R5 cells seem to use the PI3K/Akt pathway to differentiate morphologically and survive in serum-free conditions.

Expression of CD9 also inhibits production of MMP-2. MMPs, including MMP-2 and MMP-9, play a pivotal role in tumor cell invasion and metastasis (21). Indeed, motility of OS3-R5 cells was MMP dependent because a synthetic pan-MMP inhibitor, GM6001, dose-dependently inhibited migration on fibronectin-coated

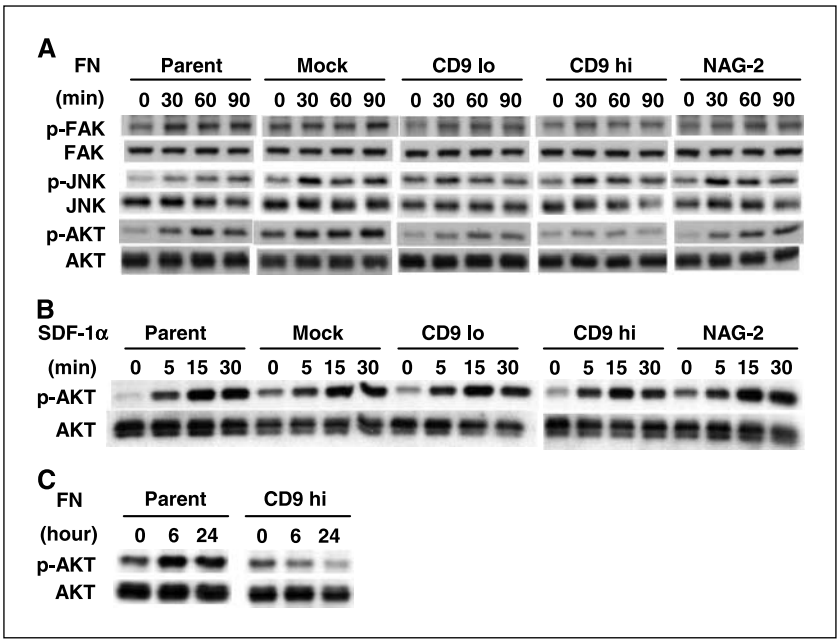

Figure 3. Postadhesive phosphorylation of Akt is attenuated in CD9 transfectants. *A,* OS3-R5 and its transfectants were cultured on fibronectin-coated dishes in serum-free conditions. After the indicated periods, these cells were lysed. Cell lysates were separated by SDS-PAGE, transferred to membranes, and probed with antibodies to FAK, JNK, and Akt, or their phosphorylated forms (*p-FAK, p-JNK*, and *p-AKT*). Representative of three independent experiments. *B,* cells were cultured on nontissue culture-treated dishes and stimulated with 100 ng/mL SDF-1α in serum-free conditions. The cells remained floating within 30 minutes in these conditions. After the indicated periods, the cells were lysed and immunoblotting for phosphorylated Akt and total Akt was done as in (*A*). *C,* cells were cultured on fibronectin for the indicated periods, and immunoblotting for phosphorylated Akt and total Akt was done as in (*A*).

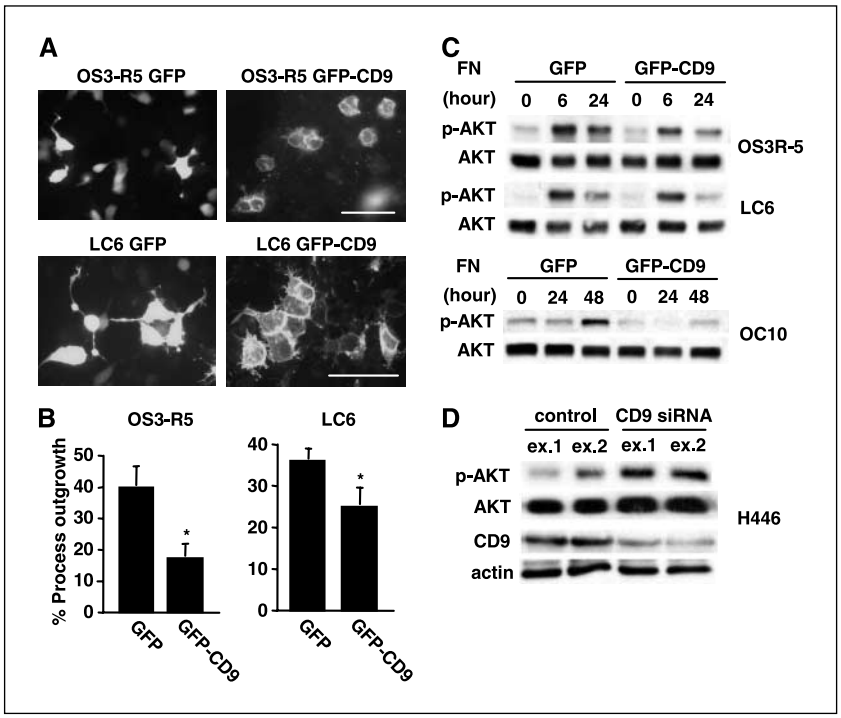

Figure 4. Transfection of SCLC cells with GFP-CD9 or siRNAs against CD9. *A,* OS3-R5 and CADO LC6 cells transiently transfected with GFP or GFP-CD9 were cultured for 6 hours on fibronectin in serum-free conditions. After fixation, the cells were visualized under a fluorescent microscope. Bar, 50 μm. *B,* percentage of cells with a process longer than 1-cell diameter was determined in (*A*). *Columns,* mean; *bars,* SD. *, $P < 0.05$. *C,* at the indicated times after the transient transfection of GFP and GFP-CD9, cell lysates of OS3-R5, CADO LC6, and OC10 were prepared, separated by SDS-PAGE, and transferred to membranes. Immunoblotting for phosphorylated Akt and total Akt was then done. *D,* NCI-H446 cells were transfected with siRNAs against CD9 or control RNAs and cultured for 72 hours on fibronectin in low-serum (1% FBS) conditions. The cells were lysed and cell lysates were fractionated on SDS-PAGE. After transfer to membranes, immunoblotting for phosphorylated Akt, total Akt, and CD9 was done. Anti-actin immunoblotting was also done to confirm the loading of comparable amounts of protein. The siRNA transfection was repeated, and similar results were obtained in the two experiments (*ex.1* and *ex.2*).

Transwell.[1] A previous study using a breast cancer cell line suggested that integrin-tetraspanin complexes regulate cell migration and MMP-2 production through PI3K/Akt pathway (12). Because CD9 expression attenuated adhesion-dependent Akt phosphorylation in SCLC cells as described above, we additionally examined whether MMP production is altered in adherent CD9 transfectants. As shown in RT-PCR analysis, transcription of MMP-2 and MT1-MMP were strongly suppressed in OS3-R5-CD9hi cells (Fig. 6*A*). Meanwhile, there was no difference in transcription of MMP-9, TIMP-1, and TIMP-2. In agreement with the decreased production of MMP-2, gelatin zymography revealed that gelatinolytic activity of pro-MMP-2 was reduced in CD9hi cells (Fig. 6*B*). Interestingly, activation of pro-MMP-2 to mature MMP-2 was enhanced in OS3-R5-NAG-2 cells; mechanisms of this prominent activation were unknown.

To examine if the PI3K pathway is involved in MMP-2 production of the parent OS3-R5, adherent cells were treated with the kinase inhibitors, including LY294002, and the activity of MMP-2 in culture supernatant was assessed by gelatin zymography (Fig. 6*C*). Because 10 μmol/L LY294002 affected the viability of OS3-R5 (Fig. 5), the concentration of LY294002 was lowered to 5 μmol/L in this experiment. Only LY294002, but not the other inhibitors, weakened the gelatinolytic band of pro-MMP-2, suggesting that the PI3K pathway is required for the MMP-2 production in OS3-R5. RT-PCR analysis revealed that the expression of MMP-2 was already reduced at the point of 24 hours after culture with LY294002 (data not shown).

We also examined transcription of MMP-2 and MT1-MMP in NCI-H446 cells after siRNA transfection against CD9. Down-regulation of CD9 in NCI-H446 seemed not to affect production of MMP-2, but it did up-regulate that of MT1-MMP (Fig. 6*D*).

[1] Y. Saito and I. Tachibana, unpublished observations.

Discussion

Invasion and metastasis of SCLC occur extremely early, and despite initial response to therapies, SCLC cells eventually acquire resistance to a broad spectrum of anticancer agents and develop into recurrent tumors (1). Mechanisms accounting for this malignant phenotype remain largely unknown. Our previous study showed that CD9, a tetraspanin almost ubiquitously present in multiple normal tissues, including the lung, and cancers, including NSCLC, is absent in SCLC, and its forced expression inhibits SCLC cell motility *in vitro* (14). Recently, it was also showed that CD9 expression in SCLC cells suppresses liver metastasis *in vivo* (22). These results suggest that the absence of CD9 may contribute to highly motile behavior of SCLC cells, leading to rapid invasion and early metastasis. The present study has proposed that the expression of CD9 is proapoptotic; thus, its absence also contributes to survival of SCLC cells.

SCLC is characterized by neuroendocrine features as evidenced by the presence of dense core granules, production of hormones and neuropeptide, and expression of N-CAM (23). Some SCLC cell lines reveal integrin-dependent neuron-like cell-shape change, and such morphologic differentiation is associated with prolonged cell survival (3, 6, 16). Consistent with these, SCLC cells examined in the present study extended long projections when adhered onto fibronectin under serum-starved conditions. Moreover, fibronectin-induced morphologic differentiation was associated with prolonged cell survival in OS3-R5, OC10, and NCI-H446. These effects were mediated by integrin β_1 receptors because adhesion to fibronectin was inhibited by anti-integrin β_1 mAb. In CADO LC6 and OS2-RA, we observed no difference in morphologic change and cell survival between fibronectin and PLL. This was probably because these cells secreted ECM proteins, including fibronectin (3), and adhered via integrins onto these proteins that overlie PLL. Indeed, we showed previously that, in serum-free conditions, CADO LC6 extended long processes even on BSA-coated wells, and

this was blocked by anti-integrin β_1 mAbs (16). Our data and previous results underscore the importance of integrin β_1–mediated signals in morphology and survival of SCLC.

We have shown that ectopic expression of CD9 suppressed the morphologic differentiation of SCLC cells. Specifically, fibronectin-induced process outgrowth was decreased in OS3-R5-CD9 stable transfectants. Moreover, transient transfection of GFP-CD9 into OS3-R5 and another line CADO LC6 compromised the process extension. The possible involvement of CD9 in neuronal differentiation has been suggested in previous studies. Anti-CD9 mAb increased neurite outgrowth in mouse cerebellar neurons (24). In addition, anti-CD9 mAb promoted neurite formation of rat sympathetic neurons in an integrin $\alpha_3\beta_1$–dependent manner (25). Because $CD9^+$ NCI-H446 morphologically differentiated as well as the $CD9^-$ lines in the present study, the absence of CD9 seems not to be essential for neuron-type morphologic differentiation. Rather, the capability of process extension in SCLC may depend on multiple factors, and based on the established concept that CD9 indirectly associates with integrins in tetraspanin-enriched microdomains (8), CD9 presumably acts as modulator of cytoskeletal reorganization. The presence of CD9 also seems to be proapoptotic for SCLC because, on serum withdrawal, TUNEL-positive cells in the OS3-R5-CD9 transfectants were twice as many as in control cells. Furthermore, a larger percentage of cells were apoptotic on fibronectin in $CD9^+$ NCI-H446 when compared with the other $CD9^-$ lines (Fig. 1*C*). Regarding CD9 expression and cell apoptosis,

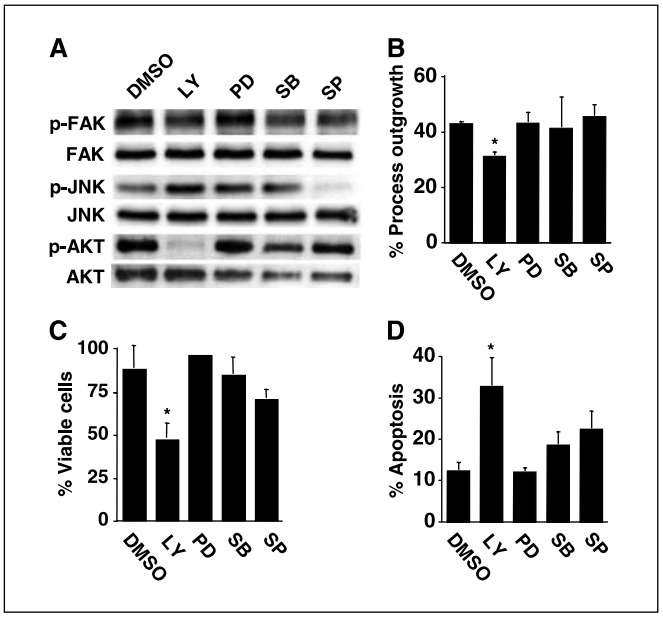

Figure 5. PI3K/Akt signaling is required for process outgrowth and survival of OS3-R5 cells. *A,* OS3-R5 cells were cultured for 90 minutes on fibronectin-coated wells in serum-free medium containing 10 μmol/L LY294002 (*LY*), 20 μmol/L PD98059 (*PD*), 10 μmol/L SB203580 (*SB*), 20 μmol/L SP600125 (*SP*), or vehicle (DMSO) alone. After the cells were lysed, lysates were separated by SDS-PAGE, transferred to membranes, and probed with antibodies to FAK, JNK, and Akt or their phosphorylated forms (*p-FAK, p-JNK*, and *p-AKT*). *B,* cells were cultured for 3 hours as in (*A*) and photographed. The percentage of cells with a process longer than 1-cell diameter was determined. *C,* cells were cultured for 72 hours as in (*A*). Viable cells were counted by trypan blue dye exclusion, and the percentage of viable cells was determined. *D,* cells were cultured for 48 hours on fibronectin-coated chamber slides in low-serum (0.1% FBS) medium containing the inhibitors. After fixation, TUNEL was done and the percentage of apoptotic cells was determined. *Columns,* mean; *bars,* SD. *, $P < 0.05$ versus DMSO.

one previous article showed that transfection of CD9 and another metastasis suppressor tetraspanin CD82 not only inhibited cell motility but also promoted apoptosis in Chinese hamster ovary mutant cells (26). Although these effects were dependent on GM3 synthesis and glycosylation state of the tetraspanins and detailed mechanisms for cell apoptosis were not clarified, this study supports our hypothesis that CD9 expression in SCLC cells exerts antitumor effects through the induction of early cell apoptosis.

PI3K-mediated signals control cytoskeletal rearrangement, cell growth, and cell survival (27). Constitutive activation of the PI3K/Akt pathway in SCLC has been reported in previous studies. Multiple mechanisms, including mutations of PTEN, expression of specific PI3K isoforms, and presence of growth factor/its receptor autocrine loops, may contribute to such constitutive activation and thus facilitate anchorage-independent growth of SCLC cells (28–30). Meanwhile, cell adhesion-dependent activation of PI3K/Akt pathway has also been increasingly highlighted in SCLC, and through this pathway, SCLC cells may be protected against chemotherapy-induced apoptosis (5, 7). We observed that Ser^{473} of Akt was constitutively phosphorylated in OS3-R5 and, more importantly, the phosphorylation level was up-regulated after adhesion to fibronectin. The activation of PI3K/Akt signaling seems to be required for morphologic differentiation and cell survival because the PI3K inhibitor LY294002, which abolished the Akt phosphorylation, inhibited process outgrowth and induced early apoptosis. Notably, we have shown that stable and transient transfection of CD9 into OS3-R5, CADO LC6, and OC10 attenuated the postadhesive phosphorylation of Akt. Down-regulation of endogenous CD9 by siRNA transfection into NCI-H446 conversely augmented the Akt phosphorylation. The interference by CD9 in Akt phosphorylation seems to be specific to cell adherence, because no difference was detected in SDF-1α-CXCR4 interaction-induced Akt phosphorylation. Given that CD9 associated with β_1 integrins, it is reasonable that CD9 specifically affects fibronectin-mediated intracellular signals, including the PI3K/Akt pathway. The interaction of CD9 with fibronectin-binding β_1 integrins may be looser than that with laminin-binding β_1 integrins (31), but several studies have shown that CD9 expression can affect cell behaviors on fibronectin (32, 33). Collectively, our data suggest that the defective postadhesive activation of PI3K/Akt is part of mechanisms involved in the suppressive effects of CD9 on SCLC cell morphology and survival.

MMPs play a crucial role in degradation of ECM and are involved in cancer invasion and metastasis. Tumor cell-ECM interactions mediated by integrins induce production of MMPs by tumor cells (21). Although mechanisms that link integrin-mediated adhesion and MMP production in tumor cells are poorly understood, it was recently suggested that tetraspanin-integrin complexes may regulate MMP-2 production by PI3K-dependent pathway. Treatment of a breast cancer cell line with anti-tetraspanin mAbs stimulated production of MMP-2 and formation of long invasive protrusions, and the PI3K inhibitor LY294002 negated these effects (12). Anti-CD9 mAb or antisense oligonucleotide against CD9 stimulated MMP-2 production of blastocysts on fibronectin in mice, and LY294002 counteracted this effect (33). In line with these previous results, the present study has shown that transfection of CD9 into SCLC cells inhibited the transcription of MMP-2 as well as MT1-MMP. Gelatinolytic activity of pro-MMP-2 was also decreased. These MMP-2 changes were clearly observed in OS3-R5-CD9hi cells but not obvious in CD9lo cells (data not shown). In addition, incomplete abrogation of CD9 expression by siRNA

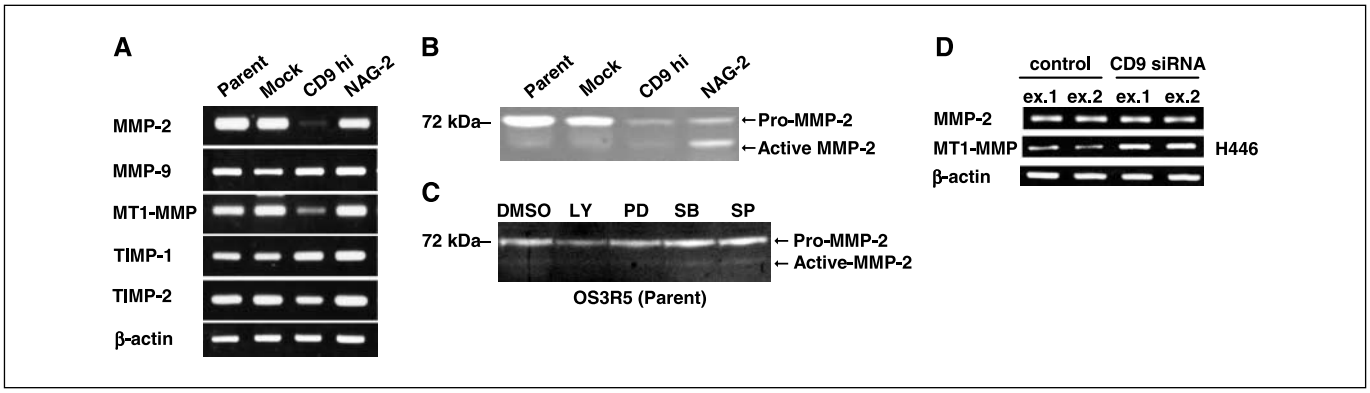

Figure 6. Expression of CD9 also inhibits production of MMP-2 and MT1-MMP. *A,* OS3-R5 and its transfectants were cultured for 48 hours on fibronectin-coated dishes in serum-free conditions. Total RNA was extracted and analyzed for expressions of MMP-2, MMP-9, MT1-MMP, TIMP-1, and TIMP-2 by RT-PCR. β-Actin amplification was used as the internal control. *B,* OS3-R5 and its transfectants were cultured for 48 hours in serum-free medium. The culture supernatants were concentrated 10-fold and resolved in SDS-PAGE containing 0.1% gelatin. The gels were incubated in developing buffer and lytic bands were visualized by Coomassie brilliant blue R250 staining. *C,* OS3-R5 cells were cultured for 48 hours on fibronectin in serum-free medium containing 5 μmol/L LY294002, 20 μmol/L PD98059, 10 μmol/L SB203580, 20 μmol/L SP600125, or vehicle (DMSO) alone. MMP-2 activity in culture supernatants was examined by gelatin zymography as in (*B*). *D,* NCI-H446 cells were transfected with siRNAs against CD9 or control RNAs and cultured for 48 hours on fibronectin in low-serum (1% FBS) conditions. Expressions of MMP-2 and MT1-MMP were analyzed by RT-PCR.

transfection in $CD9^+$ NCI-H446 cells enhanced the transcription of MT1-MMP but did not affect that of MMP-2. These may indicate the presence of a threshold in the CD9 effect on the MMP-2 expression. CD9-induced down-regulation of postadhesive PI3K/Akt activation seems to be at least partially responsible for the MMP-2 reduction in the CD9hi cells, because LY294002 inhibited MMP-2 production of the parent OS3-R5 cells. Thus, although detailed mechanisms remain elusive, suppression of MMP-2 production may be included in PI3K/Akt-dependent antitumor effects of CD9.

In conclusion, the present study has proposed that the absence of CD9 contributes to highly malignant phenotype of SCLC by conferring antiapoptotic signals in addition to the previously recognized motility-promoting effect. Moreover, activation of the PI3K/Akt pathway is most likely part of mechanisms involved. Available evidence thus far does not support CD9 gene mutation, loss of heterozygosity at the human chromosome, or promoter hypermethylation in human cancers. Thus, it might be possible to turn on the CD9 gene expression, and such a strategy would be useful in designing novel therapies for SCLC.

Acknowledgments

Received 3/27/2006; revised 6/24/2006; accepted 7/26/2006.

Grant support: Ministry of Education, Science, and Culture, Japan.

The costs of publication of this article were defrayed in part by the payment of page charges. This article must therefore be hereby marked *advertisement* in accordance with 18 U.S.C. Section 1734 solely to indicate this fact.

We thank Y. Habe for secretarial assistance.

References

1. Aisner J. Extensive-disease small-cell lung cancer: the thrill of victory; the agony of defeat. J Clin Oncol 1996;14:658–65.
2. Brambilla E, Moro D, Gazzeri S, et al. Cytotoxic chemotherapy induces cell differentiation in small-cell lung carcinoma. J Clin Oncol 1991;9:50–61.
3. Sethi T, Rintoul RC, Moore SM, et al. Extracellular matrix proteins protect small cell lung cancer cells against apoptosis: a mechanism for small cell lung cancer growth and drug resistance *in vivo*. Nat Med 1999;5:662–8.
4. Moore SM, Rintoul RC, Walker TR, Chilvers ER, Haslett C, Sethi T. The presence of a constitutively active phosphoinositide 3-kinase in small cell lung cancer cells mediates anchorage-independent proliferation via a protein kinase B and p70s6k-dependent pathway. Cancer Res 1998;58:5239–47.
5. Kraus AC, Ferber I, Bachmann SO, et al. *In vitro* chemo- and radio-resistance in small cell lung cancer correlates with cell adhesion and constitutive activation of AKT and MAP kinase pathways. Oncogene 2002;21:8683–95.
6. Kijima T, Maulik G, Ma PC, Madhiwala P, Schaefer E, Salgia R. Fibronectin enhances viability and alters cytoskeletal functions (with effects on the phosphatidylinositol 3-kinase pathway) in small cell lung cancer. J Cell Mol Med 2003;7:157–64.
7. Tsurutani J, West KA, Sayyah J, Gills JJ, Dennis PA. Inhibition of the phosphatidylinositol 3-kinase/Akt/mammalian target of rapamycin pathway but not the MEK/ERK pathway attenuates laminin-mediated small cell lung cancer cellular survival and resistance to imatinib mesylate or chemotherapy. Cancer Res 2005;65:8423–32.
8. Hemler ME. Tetraspanin functions and associated microdomains. Nat Rev Mol Cell Biol 2005;6:801–11.
9. Wright MD, Moseley GW, van Spriel AB. Tetraspanin microdomains in immune cell signalling and malignant disease. Tissue Antigens 2004;64:533–42.
10. Boucheix C, Rubinstein E. Tetraspanins. Cell Mol Life Sci 2001;58:1189–205.
11. Boucheix C, Duc GH, Jasmin C, Rubinstein E. Tetraspanins and malignancy. Expert Rev Mol Med 2001;2001:1–17.
12. Sugiura T, Berditchevski F. Function of $\alpha_3\beta_1$-tetraspanin protein complexes in tumor cell invasion. Evidence for the role of the complexes in production of matrix metalloproteinase 2 (MMP-2). J Cell Biol 1999;146:1375–89.
13. Sawada S, Yoshimoto M, Odintsova E, Hotchin NA, Berditchevski F. The tetraspanin CD151 functions as a negative regulator in the adhesion-dependent activation of Ras. J Biol Chem 2003;278:26323–6.
14. Funakoshi T, Tachibana I, Hoshida Y, et al. Expression of tetraspanins in human lung cancer cells: frequent downregulation of CD9 and its contribution to cell motility in small cell lung cancer. Oncogene 2003;22:674–87.
15. Tachibana I, Bodorova J, Berditchevski F, Zutter MM, Hemler ME. NAG-2, a novel transmembrane-4 superfamily (TM4SF) protein that complexes with integrins and other TM4SF proteins. J Biol Chem 1997;272:29181–9.
16. Tachibana I, Mori M, Tanio Y, et al. A 100-kDa protein tyrosine phosphorylation is concurrent with β_1 integrin-mediated morphological differentiation in neuroblastoma and small cell lung cancer cells. Exp Cell Res 1996;227:230–9.
17. Munaut C, Noel A, Hougrand O, Foidart JM, Boniver J, Deprez M. Vascular endothelial growth factor expression correlates with matrix metalloproteinases MT1-MMP, MMP-2 and MMP-9 in human glioblastomas. Int J Cancer 2003;106:848–55.
18. Giancotti FG, Ruoslahti E. Integrin signaling. Science 1999;285:1028–32.
19. Gu J, Fujibayashi A, Yamada KM, Sekiguchi K. Laminin-10/11 and fibronectin differentially prevent apoptosis induced by serum removal via phosphatidylinositol 3-kinase/Akt- and MEK1/ERK-dependent pathways. J Biol Chem 2002;277:19922–8.
20. Kijima T, Maulik G, Ma PC, et al. Regulation of cellular proliferation, cytoskeletal function, and signal transduction through CXCR4 and c-Kit in small cell lung cancer cells. Cancer Res 2002;62:6304–11.
21. Bjorklund M, Koivunen E. Gelatinase-mediated

migration and invasion of cancer cells. Biochim Biophys Acta 2005;1755:37–69.
22. Zheng R, Yano S, Zhang H, et al. CD9 overexpression suppressed the liver metastasis and malignant ascites via inhibition of proliferation and motility of small-cell lung cancer cells in NK cell-depleted SCID mice. Oncol Res 2005;15:365–72.
23. Carney DN, Gazdar AF, Bepler G, et al. Establishment and identification of small cell lung cancer cell lines having classic and variant features. Cancer Res 1985;45:2913–23.
24. Schmidt C, Kunemund V, Wintergerst ES, Schmitz B, Schachner M. CD9 of mouse brain is implicated in neurite outgrowth and cell migration *in vitro* and is associated with the α_6/β_1 integrin and the neural adhesion molecule L1. J Neurosci Res 1996;43:12–31.
25. Banerjee SA, Hadjiargyrou M, Patterson PH. An antibody to the tetraspan membrane protein CD9 promotes neurite formation in a partially $\alpha_3\beta_1$ integrin-dependent manner. J Neurosci 1997;17:2756–65.
26. Ono M, Handa K, Withers DA, Hakomori S. Motility inhibition and apoptosis are induced by metastasis-suppressing gene product CD82 and its analogue CD9, with concurrent glycosylation. Cancer Res 1999;59:2335–9.
27. Hennessy BT, Smith DL, Ram PT, Lu Y, Mills GB. Exploiting the PI3K/AKT pathway for cancer drug discovery. Nat Rev Drug Discov 2005;4:988–1004.
28. Yokomizo A, Tindall DJ, Drabkin H, et al. PTEN/MMAC1 mutations identified in small cell, but not in non-small cell lung cancers. Oncogene 1998;17:475–9.
29. Arcaro A, Khanzada UK, Vanhaesebroeck B, Tetley TD, Waterfield MD, Seckl MJ. Two distinct phosphoinositide 3-kinases mediate polypeptide growth factor-stimulated PKB activation. EMBO J 2002;21:5097–108.
30. Krystal GW, Sulanke G, Litz J. Inhibition of phosphatidylinositol 3-kinase-Akt signaling blocks growth, promotes apoptosis, and enhances sensitivity of small cell lung cancer cells to chemotherapy. Mol Cancer Ther 2002;1:913–22.
31. Hemler ME. Tetraspanin proteins mediate cellular penetration, invasion, and fusion events and define a novel type of membrane microdomain. Annu Rev Cell Dev Biol 2003;19:397–422.
32. Longhurst CM, Jacobs JD, White MM, et al. Chinese hamster ovary cell motility to fibronectin is modulated by the second extracellular loop of CD9. Identification of a putative fibronectin binding site. J Biol Chem 2002;277:32445–52.
33. Liu WM, Cao YJ, Yang YJ, Li J, Hu Z, Duan EK. Tetraspanin CD9 regulates invasion during mouse embryo implantation. J Mol Endocrinol 2006;36:121–30.

Absence of CD9 Enhances Adhesion-Dependent Morphologic Differentiation, Survival, and Matrix Metalloproteinase-2 Production in Small Cell Lung Cancer Cells

Yoshiyuki Saito, Isao Tachibana, Yoshito Takeda, et al.

Cancer Res 2006;66:9557-9565.